

# **Design of Optical Time-Division Multiplexed Systems Using the Cascaded Four-Wave Mixing in a Highly Nonlinear Photonic Crystal Fiber for Simultaneous Time Demultiplexing and Wavelength Multicasting**

**Zhan-Qiang Hui<sup>1,\*</sup>** and **Jian-Guo Zhang<sup>2,\*</sup>**

<sup>1</sup>School of Electronic Engineering, Xi'an University of Posts and Telecommunications  
Xi'an, Shaanxi 710121, China

<sup>2</sup>Department of Engineering and Design, School of Engineering  
London South Bank University, 103 Borough Road, London SE1 0AA, UK

## **Abstract**

This paper reports a new design of optical time-division multiplexed (OTDM) systems that possess a functionality of simultaneous time demultiplexing and wavelength multicasting based on the cascaded four-wave mixing in a dispersion-flattened highly nonlinear photonic crystal fiber (DF-HNL-PCF). A module of OTDM demultiplexing and wavelength multicasting can be feasibly implemented by using a 3dB optical coupler, a high-power erbium-doped fiber amplifier, a short-length DF-HNL-PCF, and a wavelength demultiplexer in the simple configuration. We also carry out an experiment on the proposed system to demonstrate the 100Gbit/s-to-10Gbit/s OTDM demultiplexing with wavelength conversion simultaneously at 4 multicast wavelengths. It is shown that error-free wavelength multicasting is achieved on two wavelength channels with the minimum power penalty of 3.2 dB relative to the 10Gbit/s back-to-back measurement, whereas the bit error rates of other two multicasting channels are measured to be about  $10^{-6}$  to  $10^{-5}$ . Moreover, we propose the use of a proper error-correcting code to improve the multicasting performance of such an OTDM system, and our work reveals that the resulting system can theoretically support error-free multicasting of the OTDM-demultiplexed signal on four wavelength channels.

---

\*Corresponding authors: Jian-Guo Zhang (email: [jian-guo-zhang@126.com](mailto:jian-guo-zhang@126.com)); Zhan-Qiang Hui (mail: [zhanqianghui@xupt.edu.cn](mailto:zhanqianghui@xupt.edu.cn)). Experimental research was carried out by Z.-Q. Hui at the State Key Laboratory of Transient Optics and Photonics at Xi'an Institute of Optics and Precision Mechanics of CAS; while error correcting codes in OTDM systems were theoretically studied by J.-G. Zhang at London South Bank University.

**Keywords:** Optical fiber communications, optical time-division multiplexing, wavelength multicasting, four-wave mixing, photonic crystal fiber, error-correcting code, optical nonlinearity.

## 1. Introduction

With applications of cloud computing, high-definition (HD) and/or three-dimensional TV, video conferencing, HD video-on-demand and online real-time gaming, global Internet traffic has been growing rapidly in recent years [1]. Consequently, there is an increasing demand for ultrahigh-capacity optical fiber communication systems in order to effectively support the bandwidth-intensive applications [2]. In general, optical time-division multiplexing (OTDM) and dense wavelength-division multiplexing (WDM) are regarded as two feasible techniques that can be used to achieve ultrahigh-speed and high-capacity optical data communications in fiber-optic systems/networks. Fundamentally, both multiplexing techniques are distinct in their operational principles. OTDM employs ultrashort optical pulse signals and optical delay lines to perform an optical time-domain multiplexing at the transmitting end and uses ultrafast optical-time demultiplexers to extract optical data signals from individual OTDM channels at the receiving end [2]-[7]. This in turn allows all the channels to send out their data signals (having identical data bit rate of  $B_d$  and the same wavelength) in the serial-transmission manner over a common single-mode fiber at an aggregate bit rate that is normally much higher than  $B_d$ . In contrast, WDM is based on the parallel transmission of multiple channel data at distinct wavelengths over a common optical fiber, so that the ultrahigh capacity of a dense WDM system is

achieved by multiplexing all the channel data signals in the optical wavelength domain. From the viewpoint of system design and operation, a main advantage of OTDM over dense WDM is the reduction of management effort, complexity, power consumption and cost per bit for high-capacity optical fiber communications [4].

Since optical time demultiplexing is one of key functions to build OTDM systems, there has been intensive research on the implementation of OTDM demultiplexers using optical nonlinearities [2]-[10]. For example, such demultiplexers can utilize cross-phase modulation (XPM) and four-wave mixing (FWM) in semiconductor optical amplifier (SOA) [8][9] and a variety of optical fibers [3]-[7][10]-[17], respectively. However, the operation speed of SOA-based demultiplexers can be ultimately limited by the relatively long gain recovery time in SOAs, and the amplified spontaneous emission noise of a SOA can also cause the degradation of the demultiplexed data signal. On the other hand, optical fibers are mature for massive production with low cost and possess the femtosecond response time of Kerr nonlinearity. Moreover, OTDM demultiplexers based on optical fibers can have a low coupling loss when they are connected with transmission fibers or other fiber-based devices in photonic communication systems or networks. Unfortunately, the long interactive length is required by a dispersion-shifted fiber (DSF) with low nonlinear coefficient in order to obtain sufficient optical nonlinear effect. This in turn leads to a bulky OTDM demultiplexer which can be sensitive to environmental disturbances (e.g., temperature drift and acoustic effect). Such a problem, however, can be solved by employing a highly nonlinear fiber (HNLF) with the shortened length to replace a DSF in the OTDM

demultiplexer [10][11]. Although the operation stability of the resulting demultiplexer is improved, a walk-off between optical pulses or a phase mismatch due to dispersion in traditional HNLFs can still restrict the operational wavelength range of HNLF-based demultiplexers. By utilizing FWM in silicon nanowire [18] and chalcogenide glass waveguide [19], two novel OTDM demultiplexers have been demonstrated recently, which are capable of ultrahigh-speed operation and are very promising for use in the future OTDM systems. These advanced photonic devices, however, require a sophisticated fabrication process which can prevent them from practical applications nowadays. Moreover, the reported silicon and chalcogenide waveguides also have a large coupling loss when they are connected with fiber-based devices in photonic communication systems/networks.

From the above discussions, one can see that the use of optical fibers for ultrafast time demultiplexing appears to be a cost-effective and practical solution to OTDM applications [3]-[7]. As a result, the main design concern is to minimize the effect of walk-off or phase mismatch due to the group velocity dispersion of a single-mode fiber. To design the fiber-based OTDM demultiplexer, it is highly desired to use a short-length nonlinear fiber with high nonlinear coefficient, low and very flat dispersion over a wide wavelength range. This requirement can be effectively met by employing a new type of optical fibers which are commercially available, namely, dispersion-flattened highly nonlinear photonic crystal fiber (PCF) [20]-[23]. Although PCF-based OTDM demultiplexers were demonstrated by exploiting XPM in the PCF [13]-[15] and optical logic gates using a triple-core PCF were also theoretically studied [24], they did not

have a capability of wavelength multicasting. On the other hand, there has been an intensive research on the use of PCFs for wavelength conversion and multicasting [22][23][25]-[27], respectively, while OTDM demultiplexing was not considered in such reported works. With the increasing demand on video conferencing, HDTV distribution, and HD video-on-demand, WDM networks are required to possess an important function of wavelength multicasting that allows the same data signal to be transmitted at multiple selected wavelengths and to be distributed over the network to multiple destinations [2][23][25]-[30]. If we can improve the design of conventional OTDM demultiplexers by providing an additional function of wavelength multicasting with no increase of complexity, the applicability of OTDM networks should be enhanced. At the egress of such an OTDM network, the optical time-demultiplexed signal can be replicated on multiple wavelength channels which are ready to be distributed over a WDM access network to multiple destinations. In doing so, this can simplify the optical interface at a network egress that links an OTDM core network with WDM access network(s), because all-optical wavelength multicasting is realized simultaneously during the demultiplexing of OTDM channel data.

At present, there are a few reported works on the wavelength multicasting of OTDM-demultiplexed data signals. In [16], Bres *et al* demonstrated the wavelength multicasting of an ultrahigh-speed OTDM signal followed by the OTDM demultiplexing, but two separate HNLFs were employed in multicasting and demultiplexing blocks, respectively. Moreover, the wavelengths of OTDM signal and control lights should be normally selected in the vicinity of a zero-dispersion

wavelength of the used HNLF in order to minimize the effect of phase mismatch or walk-off between control and signal pulses. Although we previously reported the use of XPM and FWM in two PCFs for 80Gbit/s wavelength conversion and 80Gbit/s-to-10Gbit/s OTDM demultiplexing with 1-to-2 wavelength multicasting [17], respectively, the resulting OTDM demultiplexer was able to offer only 2-channel wavelength multicasting. A recent work has revealed that the number of available wavelength-multicasting channels can be doubled by using the cascaded FWM in a dispersion-flattened highly nonlinear PCF (DF-HNL-PCF) for OTDM demultiplexing [31]. That reported work, however, focused on the experimental study of such an OTDM demultiplexer with no consideration of system design and performance improvement [31], in which error-free multicasting was achieved only on two of the obtained four wavelength channels. Thus, the number of usable multicasting channels is still restricted to 2. From the viewpoint of bandwidth-intensive services, the required number of multicasting channels can be more than 2 for practical communication applications. To achieve it, we present a new design of OTDM systems with a functionality of simultaneous time demultiplexing and wavelength multicasting in this paper. The proposed scheme is simple and requires only a single control-pulse light source for wavelength multicasting on  $M$  multicast channels ( $M \geq 4$ ), by using the cascaded FWM in a DF-HNL-PCF at our designed module of *OTDM demultiplexing & wavelength multicasting* and employing a proper error-correcting code to improve the multicasting performance, respectively. In our previous experiment [17], the 10GHz optical clock pulse train, which was employed at an OTDM transmitter, directly served

as a control light for OTDM demultiplexing and wavelength multicasting at the receiving end. In this paper, we use an alternative approach to provide the control light by the wavelength conversion of a 10GHz optical clock pulse train through supercontinuum generation in a dispersion-shifted HNLF. Moreover, error-correcting codes have not yet been utilized to improve the performance of special OTDM systems with function of wavelength multicasting until now. Therefore, we will study this issue subsequently. In section 2, the operational principle of the proposed scheme for demultiplexing and multicasting is described. In Section 3, we present the detailed design of an OTDM system with the required functionality of OTDM demultiplexing and wavelength multicasting. To validate the proposed design, we also demonstrate an experiment on 100Gbit/s-to-10Gbit/s OTDM demultiplexing together with 1-to-4 wavelength multicasting. Error-free data multicasting is achieved on two wavelength channels. Therefore, in Section 4 we propose to use an error-correcting code in the OTDM system with a functionality of simultaneous time demultiplexing and wavelength multicasting to ensure error-free operation on those four multicasting channels. For this purpose, we carry out a theoretic study only.

## **2. Operational Principle of the Proposed Scheme for OTDM Demultiplexing and Wavelength Multicasting**

The cascaded FWM in a single DF-HNL-PCF can be employed to realize a functionality of simultaneous time demultiplexing and wavelength multicasting in an ultrahigh-speed OTDM system. Figure 1 illustrates the conceptual design and block

diagram of an all-optical module using the proposed scheme, where  $\lambda_s$ ,  $\lambda_c$ , and  $\lambda_{F-j}$  are the central wavelengths of OTDM signal light, control-pulse light, and FWM component  $j$  for  $j = 1, 2, \dots, M$ , respectively. Since only a single control light is required and a short DF-HNL-PCF is employed, this can result in a simple configuration for the designed module of time demultiplexing and wavelength multicasting.

From the viewpoint of engineering applications, a low-cost design is highly desirable. To achieve this goal, we can use the commercially available optical components to realize an optical module of OTDM demultiplexing and wavelength multicasting. Figure 1(b) shows a feasible scheme to implement the module which consists of a 3dB optical coupler, a high-power erbium doped fiber amplifier (EDFA), a short-length PCF with high nonlinear coefficient, low and very flat dispersion, and a wavelength demultiplexer, respectively. Thus, our constructed optical module has a low complexity for implementation. Its operational principle can be described in the following.

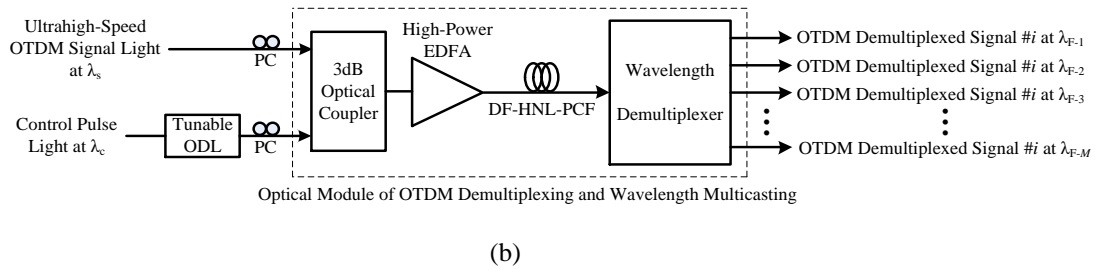
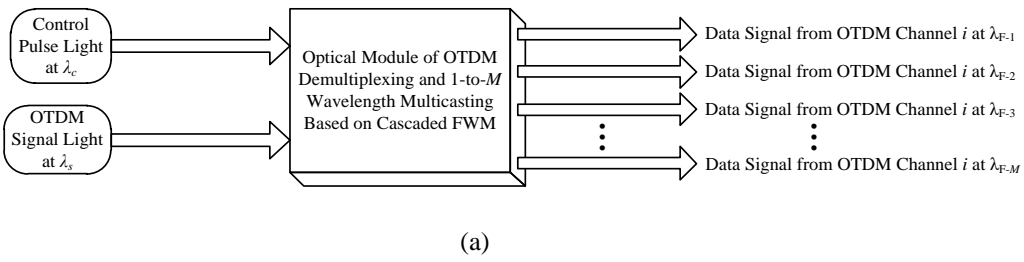


Figure 1: (a) Illustration of an all-optical module using the proposed scheme for simultaneous time demultiplexing and wavelength multicasting. (b) A feasible implementation based on commercially available optical devices.

For convenience, let  $\nu_s$  and  $\nu_c$  be the frequencies of OTDM signal and control lights, respectively. There are  $K$  data channels for optical time-division multiplexing, and each of them has a data bit rate of  $B_d$ . The data bit period  $T_d$  is equal to  $1/B_d$ . Thus, the bit rate of an OTDM signal,  $B_s$ , is expressed as  $B_s = KB_d$ . To optically demultiplex the  $i$ th-channel OTDM data signal for  $i \in [1, K]$ , the optical control pulse sequence must have a repetition rate  $f_c$  being equal to  $1/T_d = B_d$  and is adjusted to synchronize with the time slot of the selected OTDM channel by using a tunable optical delay line (ODL), as illustrated in Figures 1(b) and 2, respectively. Moreover, two polarization controllers (PCs) are employed to adjust the polarization states of OTDM signal and control lights at the input of a 3dB optical coupler in order to maximize the FWM efficiency in a DF-HNL-PCF. Subsequently, both control pulse and ultrahigh-speed OTDM signal lights with two different wavelengths are combined by a 3dB optical coupler and are also optically amplified to the proper power levels before they are fed into a short-length DF-HNL-PCF. Owing to the sufficiently high light intensity, the power-dependent refractive index of an optical fiber is resulted, which has an origin in the third-order nonlinear susceptibility [32]. This leads to a FWM interaction process between OTDM-signal and control lights, and therefore, generates the new waves.

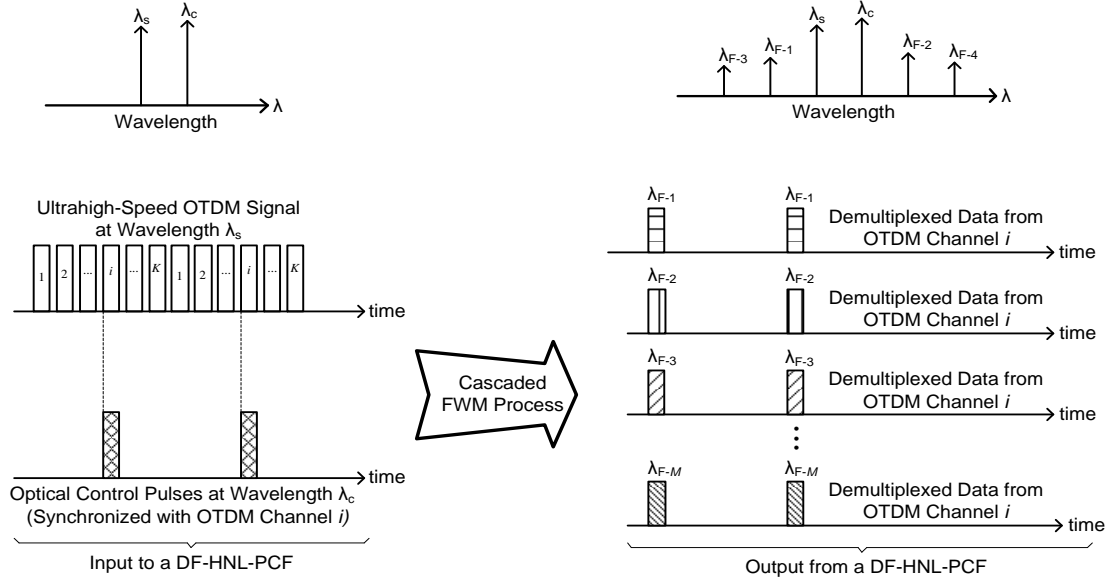


Figure 2: Illustration of 1-to- $M$  wavelength multicasting of the time-demultiplexed optical data signal from OTDM channel  $i$  by using the cascaded FWM.

A phase-matching condition must be satisfied to make FWM efficient. This is feasibly achieved in our design by using a short-length DF-HNL-PCF with low and very flat dispersion over a wide wavelength range in the 1550nm region. However, a conventional FWM interaction process between control pulse and data signal (on the selected OTDM channel) leads to the generation of the first-order FWM components at two new optical frequencies  $\nu_{F-1} = 2\nu_s - \nu_c$  and  $\nu_{F-2} = 2\nu_c - \nu_s$ , respectively. As a result, the number of wavelength multicasting channels is limited to 2 after OTDM demultiplexing. To improve the wavelength-multicasting capability without increasing the complexity, a new design is presented for the OTDM demultiplexer, which is based on the use of the cascaded FWM process. When the powers of OTDM-signal and control-pulse lights become higher in a DF-HNL-PCF, both lights can serve as two intense pump waves which initiate the cascaded FWM process in the nonlinear fiber to

produce additional wavelengths under the phase-matching condition [33]-[36]. In this case, not only FWM between the control pulse and the data signal on the selected OTDM channel generates the first-order FWM components in a DF-HNL-PCF, but also FWM among the OTDM signal, control pulse, and their FWM products can result in the generation of new waves at different optical frequencies of  $\nu_{F-j}$  for  $j = 3, 4, \dots, M$ , respectively. The cascaded FWM process can be simply understood in such a way that two strong incident fields at  $\nu_s$  and  $\nu_c$  make a refractive index moving grating that is temporally modulated at the beat frequency [34]

$$\Delta\nu = \nu_s - \nu_c \quad (1)$$

If any wave at an optical frequency of  $\nu$  propagates in the corresponding optical fiber, it would be inelastically diffracted by the grating at the frequencies of  $\nu \pm \Delta\nu$ . When these waves propagate in the nonlinear fiber, they can be further diffracted to produce new waves at other frequencies  $\nu + n \Delta\nu$ , where  $n (= \pm 1, \pm 2 \dots)$  is an integer [34][35]. The readers may refer to Refs. [36] and [37] for more detailed discussions on the complicated FWM combinations to produce higher-order components via cascaded FWM.

From the above descriptions, we can see that a FWM-resultant pulse would be produced only if both optical control pulse and OTDM signal pulse are simultaneously present in a given time slot; otherwise no pulse would result from FWM products in the nonlinear fiber. Therefore, an all-optical “logical AND” operation is achieved, with which the optical data signal on the selected  $i$ th OTDM channel is time demultiplexed and simultaneously appears at  $M$  different wavelengths  $\lambda_{F-j}$  ( $j = 1, 2, 3, \dots, M$ ) through

cascaded FWM, as illustrated in Figure 2. Now the 1-to- $M$  wavelength multicasting of the time-demultiplexed optical data signal is realized at our designed module. Then we can simply use a wavelength demultiplexer at the DF-HNL-PCF output to obtain the replicated data signals from  $M$  multicast channels at  $\lambda_{F,j}$  individually.

### **3. System Design and Experimental Demonstration**

In this section, we present the new design of an OTDM system with a functionality of simultaneous time demultiplexing and wavelength multicasting by using the optical module proposed in the above. We also report an experimental demonstration of 100Gbit/s-to-10Gbit/s OTDM demultiplexing with simultaneous wavelength multicasting on 4 channels to validate the proposed design. Here the limitation to the bit rate of an OTDM signal is due to the bandwidth of our measurement system (comprising an electrical sampling oscilloscope and a photodetector) available at the laboratory, as will be described subsequently. With the maximum bandwidth of about 70 GHz for waveform/eye-diagram measurement, we have to restrict the bit rate of an OTDM signal to  $\sim 100$  Gbit/s in the experiments. However, our designed OTDM system is capable of operating at an ultrahigh speed well beyond 100 Gbit/s, because of using fiber-based ultrafast time demultiplexing [3]-[7].

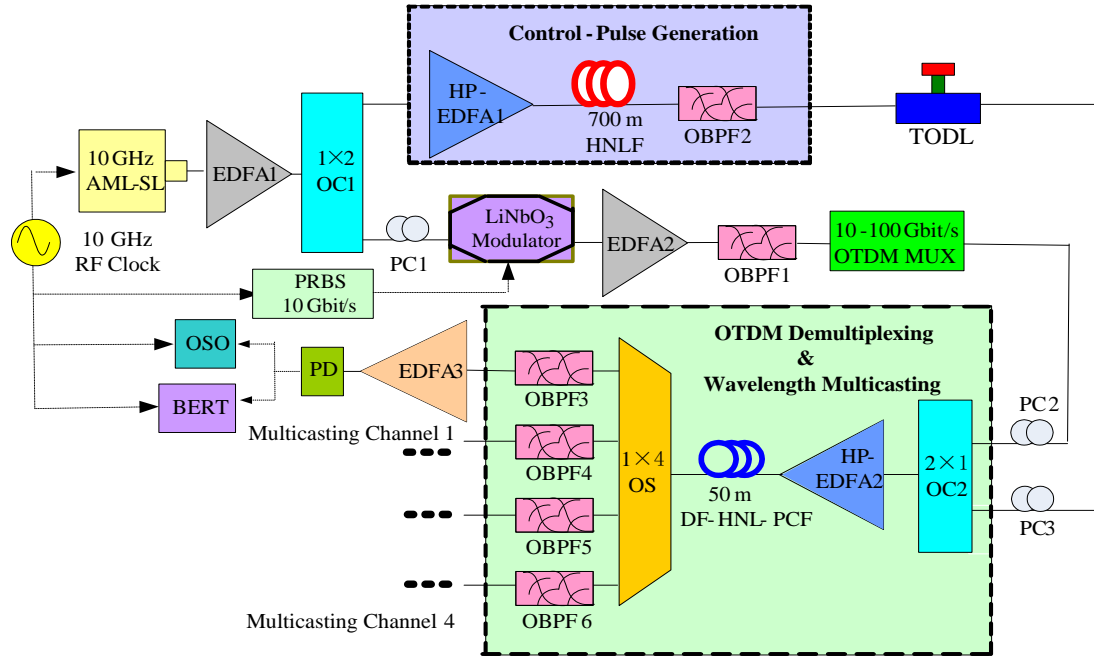
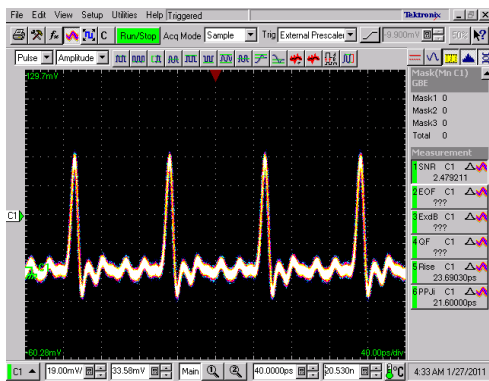


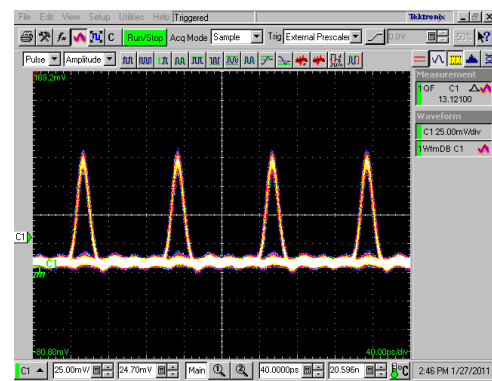
Figure 3: Experimental setup of an OTDM system with a functionality of time demultiplexing and 1-to-4 wavelength multicasting by using the proposed module based on the cascaded FWM in a DF-HNL-PCF.

An actively mode-locked semiconductor laser (AML-SL) is used as an optical clock source to produce a 10GHz optical clock-pulse train at the wavelength of 1550.31 nm. The full width at half maximum (FWHM) of the generated pulse is 1.9 ps. After optical amplification, a train of ultrashort optical clock pulses is split into two parts via a 1×2 optical coupler (OC). One of them is modulated at 10 Gbit/s by a LiNbO<sub>3</sub> Mach-Zehnder intensity modulator with an electronic  $2^{31}-1$  pseudorandom binary sequence (PRBS) in the return-to-zero (RZ) format. Then the 10Gbit/s optical data signal with pulse FWHM of 1.9 ps is fed into a fiber-based time-division multiplexer (MUX) that performs the “splitting-delay-combination” processing to generate an OTDM signal at 100 Gbit/s and 1550.31 nm for use in our experiments. The optical insertion losses of LiNbO<sub>3</sub> modulator and passive optical multiplexer are also compensated by means of

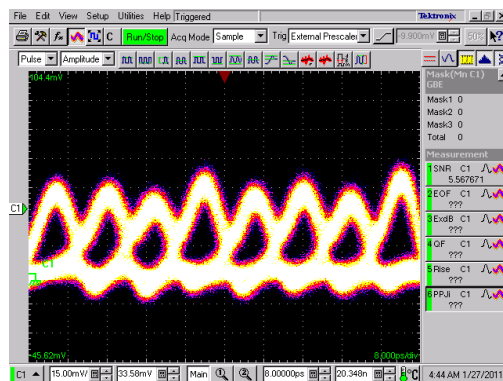
amplifying the 10Gbit/s optical data signal at EDFA 2 of which the output amplified spontaneous emission noise is effectively suppressed by an optical bandpass filter (OBPF) with 3dB bandwidth of 1.8 nm. Subsequently, we can use a 70GHz electrical sampling oscilloscope (OSO) cascaded with a 70GHz photodetector (PD) to monitor the outputs of an AML-SL, a LiNbO<sub>3</sub> intensity modulator, and a fiber-based OTDM multiplexer, respectively. The measured results are shown in Figure 4, and a small peak-power variation of OTDM signal pulses can be seen due to the use of an imperfect OTDM multiplexer in our experiment. Moreover, the eye diagram of a 100Gbit/s optical RZ signal is not resolved and the width of the displayed clock pulse is also much wider than 1.9 ps, because of the limited bandwidth (~ 70 GHz) of our measurement system.



(a)



(b)



(c)

Figure 4: (a) Waveform of the obtained 10GHz optical clock-pulse sequence from an AML-SL. (b) and (c) Eye diagrams of the measured 10Gbit/s optical RZ data and 100Gbit/s OTDM RZ signal, respectively.

The wavelengths of OTDM-signal and control lights are required to be distinct for FWM in a nonlinear fiber, while only one actively mode-locked laser is available throughout our experiment. To solve this problem, we need to change the wavelength of the split clock-pulse light from 1550.31 nm to  $\lambda_c$ . In doing so, a high-power EDFA (HP-EDFA 1) is employed to amplify the 10GHz optical clock-pulse train at the input of a 300m-long dispersion-shifted highly nonlinear fiber (DS-HNLF), so that the power of the launched clock light is 27 dBm and is sufficiently high to create supercontinuum (SC) effect in the DS-HNLF. In our experiment, the employed DS-HNLF has a nonlinear coefficient of  $9 \text{ W}^{-1} \text{ km}^{-1}$ , a dispersion of  $-2.42 \text{ ps}/(\text{nm km})$  at 1550 nm, a dispersion slope of  $0.02 \text{ ps}/\text{nm}^2 \text{ km}$ , and an attenuation coefficient of  $0.43 \text{ dB}/\text{km}$ . The SC generation leads to broadening the spectrum of the clock-pulse light which is measured by an optical spectrum analyzer (OSA, Yokogawa-AQ6370) of resolution 0.02 nm, as shown in Figure 5. Then a tunable optical bandpass filter (OBPF 2, Santec model OTF-950) with 3dB bandwidth of 1.0 nm is used at the DS-HNLF output to filter out the resulting SC spectrum at 1556.5 nm in order to produce a 10GHz optical control-pulse train. In this case, the generated SC spectrum can be considered to be nearly flat in the vicinity of 1556.5 nm with respect to a 1.0nm passband of the employed OBPF. As a result, the optical spectrum of the obtained control-pulse light is actually determined by the filtering characteristic of OBPF 2 in our experiment. The waveform

of the resulting optical control-pulse train is measured by using a 70GHz electrical sampling oscilloscope cascaded with a 70GHz photodetector and is shown in Figure 6(b), which still has a good quality compared with the original clock-pulse waveform [see Figure 6(a)]. Owing to a limited bandwidth (about 70 GHz), the measurement system has a low resolution to display the waveforms of optical control and original clock pulses, so that a difference between the widths of the measured control and clock pulses is insignificant in Figure 6. Note that the actual FWHM of the optical clock pulse is 1.9 ps and is shorter than that observed in Figure 6(a). Moreover, we focus on validating the operational principle of our proposed scheme in this paper. Consequently, we use a simple approach to distribute an optical control-pulse train in the experimental setup. That is to say, two separate optical fibers are employed for the delivery of both optical control-pulse train and OTDM signal to the designed module of OTDM demultiplexing and wavelength multicasting (see Figure 3), respectively. It would be feasible to do so if an optical control-pulse generator is located at the receiving end or a distance between transmitting and receiving ends is short. Otherwise control-pulse light at  $\lambda_c$  and OTDM signal at  $\lambda_s$  can be simultaneously transported over a common transmission fiber from the sending end to the receiving end by means of wavelength-division multiplexing. Then a WDM demultiplexer is employed to separate the control-pulse light from the OTDM signal, followed by a tunable optical delay line (TODL) to adjust the phase of an optical control-pulse train in order to coincide with the OTDM signal on the desired channel, as illustrated in Figure 7. This can be regarded as a more realistic approach than the above one to distribute an optical control-pulse train along

with the OTDM signal in an optical fiber transmission system with relatively short or medium distance (e.g., in the local-access environment), since an optical control-pulse generator can be practically located at the transmitting end. Alternatively, we can employ a sophisticated optical clock-recovery scheme that is based on actively mode-locked fiber (or semiconductor) laser and optoelectronic phase-locked loop to produce a control-pulse light of wavelength  $\lambda_c$  at the receiving end [38][39]. For long-haul OTDM applications, the optical clock-recovery scheme is more suitable than the above two approaches. However, this is achieved at the expense of high system complexity and cost. Note that the detailed discussions on generation and distribution of an optical control-pulse train are beyond the scope of this paper and will be studied in our future work.

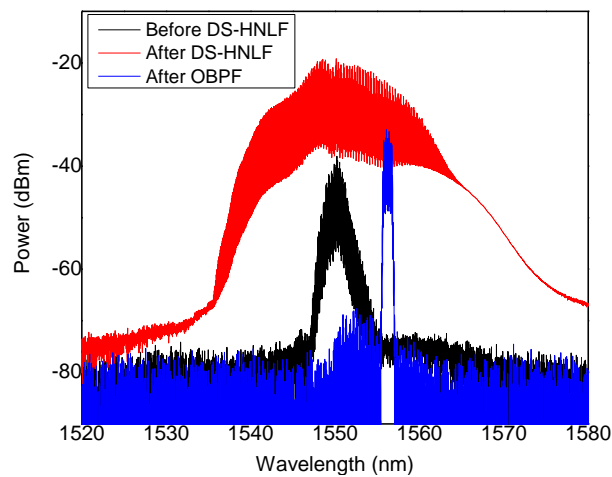
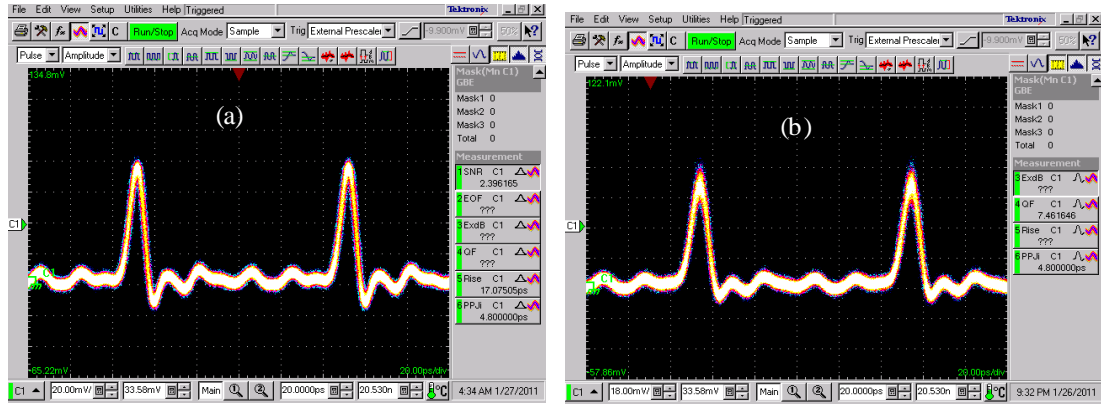


Figure 5: Optical spectra of original clock-pulse light (black trace), SC (red trace), and control-pulse light (blue trace) measured at the input & output of a DS-HNLF and after subsequent filtering, respectively.



(a)

(b)

Figure 6: Waveforms of (a) original optical clock pulses and (b) the SC-resulting control pulses measured by using a 70GHz electrical sampling oscilloscope cascaded with a 70GHz photodetector.

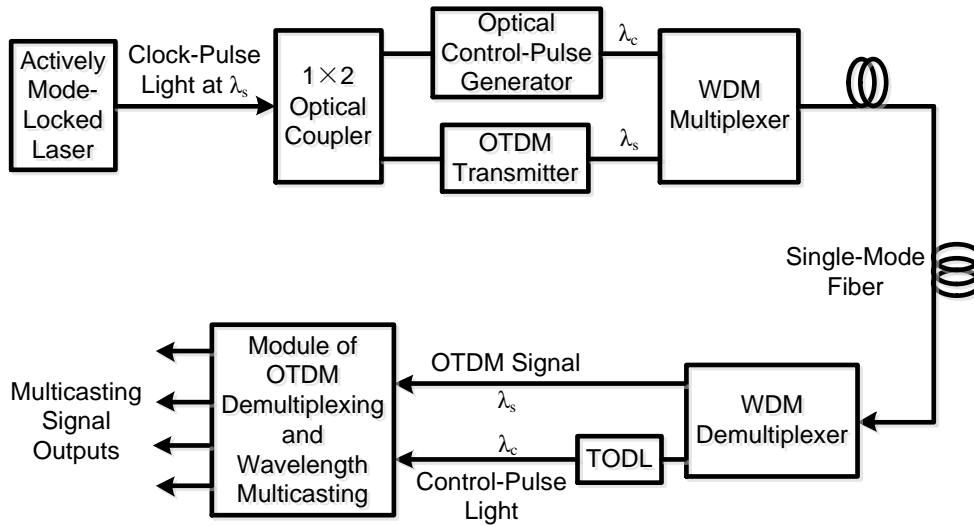


Figure 7: Illustration of a feasible approach for transmission of an optical control-pulse train along with the OTDM signal by using WDM.

At the input of an optical module of OTDM demultiplexing and wavelength multicasting, a tunable optical delay line is used to align the incoming 10GHz control pulse train with the time slot of the selected OTDM channel (see Figures 2 and 3). Two polarization controllers are also employed to adjust the polarization states of OTDM

signal and control lights for the optimization of FWM in a DF-HNL-PCF. Then 100Gbit/s OTDM signal at 1550.31 nm and 10GHz optical control pulse train at 1556.5 nm are combined by a 3dB optical coupler. To create the cascaded FWM effect in a nonlinear fiber, both OTDM and control lights are amplified by a high-power EDFA (i.e., HP-EDFA 2) to ensure the sufficiently high powers for both lights before they are launched into a DF-HNL-PCF with length of 50 m. In this experiment, the average power of the combined OTDM and control lights is 24.7 dBm, which is measured at the output of HP-EDFA 2. The DF-HNL-PCF has a nonlinear coefficient of  $11 \text{ W}^{-1} \text{ km}^{-1}$  and an attenuation coefficient of 9 dB/km. Both ends of the photonic crystal fiber are spliced to single-mode fibers, resulting in a total loss of about 1 dB. This DF-HNL-PCF has a low and very flat dispersion of  $\sim 1.25 \text{ ps nm}^{-1} \text{ km}^{-1}$  with a variation being smaller than  $0.25 \text{ ps nm}^{-1} \text{ km}^{-1}$  from 1500 nm to 1610 nm, which in turn can facilitate to minimize the effect of phase mismatch or walk-off between optical control and OTDM signal pulses. Consequently, the use of a short-length DF-HNL-PCF can ensure a wider operational wavelength range for the designed module of OTDM demultiplexing and wavelength multicasting than that of a conventional HNLF. In practice, the former also has a high flexibility of operation by eliminating the requirement of selecting the wavelengths of OTDM and control lights in the vicinity of a zero-dispersion wavelength of the optical fiber as normally encountered in the HNLF-based OTDM demultiplexers. Under the phase-matching condition, FWM between the control pulse at 1556.5 nm and the data signal (on the selected OTDM channel) at 1550.31 nm is induced in a 50m DF-HNL-PCF. Owing to sufficiently high powers for OTDM and

control lights, a cascaded FWM process in the DF-HNL-PCF results in the generation of four significant new waves at the wavelengths of  $\lambda_{F-1}$ ,  $\lambda_{F-2}$ ,  $\lambda_{F-3}$  and  $\lambda_{F-4}$ , respectively, as indicated in Figure 8. Therefore, it is clear that the same OTDM-demultiplexed signal at 10Gbit/s is multicast over four wavelength channels. At the output ports of an optical splitter (OS), we use a bank of 4 tunable OBPFs (Santec model OTF-300-004-S3) with 3dB bandwidth of 0.38 nm to extract four multicasting signals individually by tuning the central wavelengths of those OBPFs to  $\lambda_{F-1}$ ,  $\lambda_{F-2}$ ,  $\lambda_{F-3}$ , and  $\lambda_{F-4}$ , respectively. After optical amplification and subsequent photodetection, the eye diagram and bit error rate (BER) of a 10Gbit/s multicasting signal are measured by connecting the output of a 70GHz photodetector to the input ports of an electrical sampling oscilloscope and a BER tester (Anritsu model number MP1800a), respectively, as illustrated in Figure 3. Note that an alternative design of the output stage for the proposed optical module is to replace four tunable OBPFs and a 1×4 optical splitter by an integrated 4-channel wavelength demultiplexer (e.g., an arrayed waveguide grating). In doing so, this can lead to a simpler configuration and more cost-effective implementation for the optical module of OTDM demultiplexing and wavelength multicasting. Unfortunately, we do not have such a suitable wavelength demultiplexer for use in our experiments and will consider this improved design only in our future work.

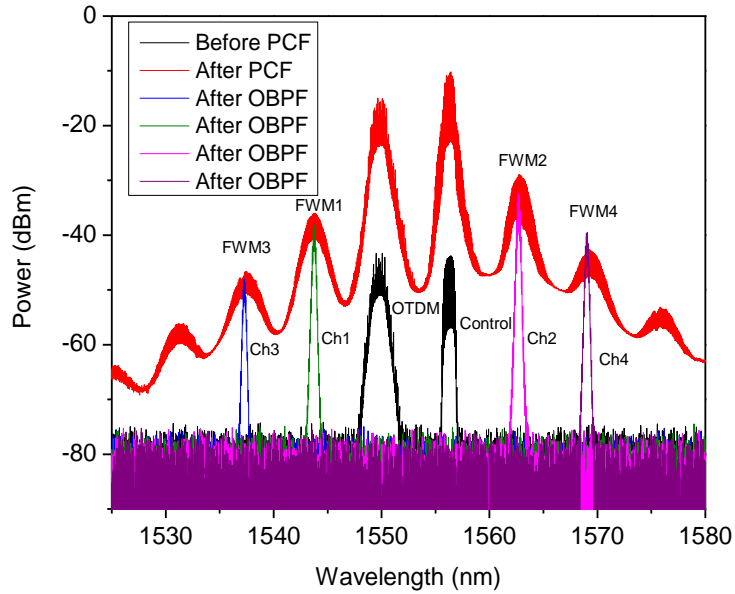


Figure 8: The measured optical spectra at the input and output of a 50m DF-HNL-PCF and the outputs of four OBPFs, respectively. Ch: Channel.

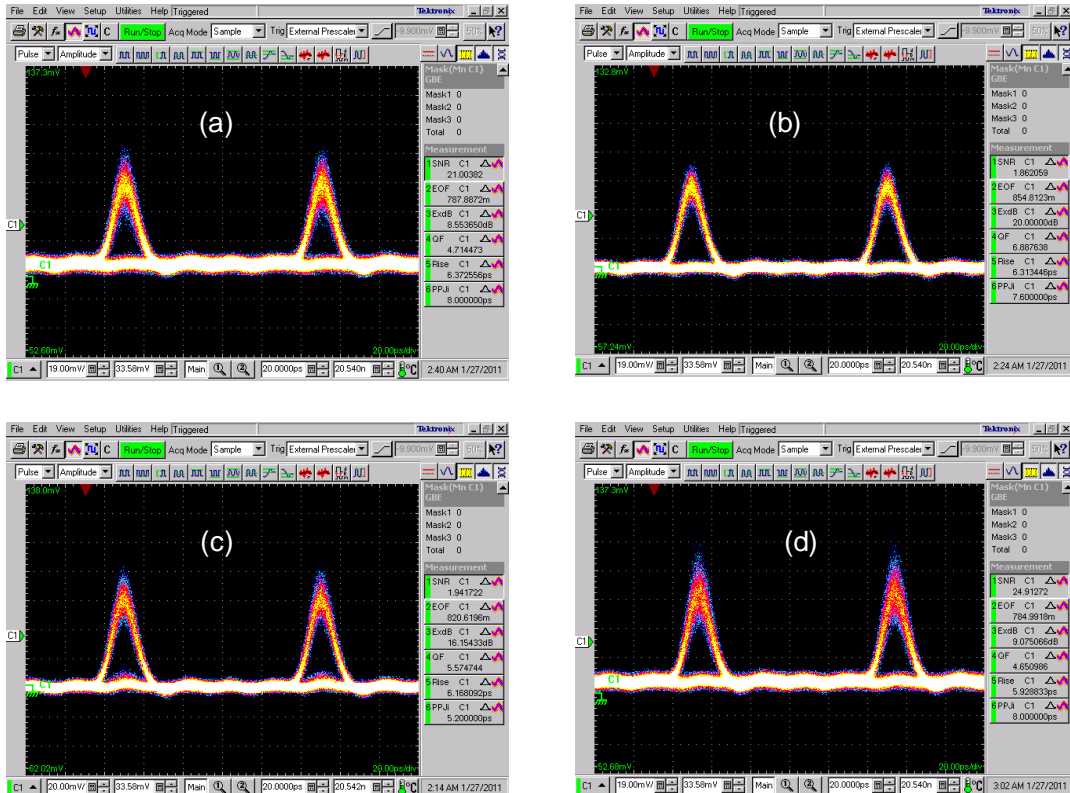


Figure 9: Eye diagrams of the 10Gbit/s OTDM-demultiplexed signal on 4 wavelength-multicasting channels at (a)  $\lambda_{F-3}=1537.21$  nm, (b)  $\lambda_{F-1}=1543.75$  nm, (c)  $\lambda_{F-2}=1562.67$  nm, and (d)  $\lambda_{F-4}=1569.05$  nm, respectively.

Figure 9 shows the eye diagrams of the multicast 10Gbit/s data signals from 4 wavelength channels measured at the output of our constructed module of OTDM demultiplexing and wavelength multicasting. After OTDM demultiplexing, clear and open eyes are observed for all four multicasting signals without showing intersymbol interference. Figure 10 indicates the BER against the optical power of each multicast data signal received by a 70GHz photodetector. It can be seen that the error-free multicasting of an OTDM demultiplexed signal is achieved on the first two wavelength channels (i.e., at  $\lambda_{F-1}$  and  $\lambda_{F-2}$ ) with the minimum power penalty of 3.2 dB at a  $10^{-9}$  BER relative to the 10Gbit/s back-to-back (BTB) measurement. This penalty can be attributed to arising from the combination of the imperfect OTDM multiplexer, EDFA noise, and pulse broadening through OBPF. However, the other two multicasting channels at  $\lambda_{F-3}$  and  $\lambda_{F-4}$  suffer from a high BER at the level of  $10^{-6}$  to  $10^{-5}$ . It is because the second-order FWM products are used and the optical signal-to-noise ratio is degraded. Moreover, there is a significant spectral overlapping between two multicast signals at  $\lambda_{F-2}$  and  $\lambda_{F-4}$ , as observed from Figure 8. Actually, multicasting channel 2 has a much higher optical power than multicasting channel 4 does. Therefore, a severe crosstalk from the adjacent channel is induced on multicasting channel 4, which could not be eliminated by optical filtering. To alleviate the crosstalk effect on the desired multicast signal, in the experiment we used the tunable OBPF with a 3dB bandwidth of 0.38 nm and a high roll-off rate outside the passband to extract the replicated 10Gbit/s optical signal at the output of an optical splitter (see Figure 3). Due to the severe

crosstalk, the BER for multicast signal 4 is worst among those four wavelength channels, even though the FWM product at  $\lambda_{F-4}$  has a higher optical power than that at  $\lambda_{F-3}$  does. Nevertheless, we will subsequently report a theoretical study to show that the use of a proper error-correcting code can ensure error-free multicasting of the OTDM demultiplexed signal on those two wavelength multicasting channels at  $\lambda_{F-3}$  and  $\lambda_{F-4}$ .

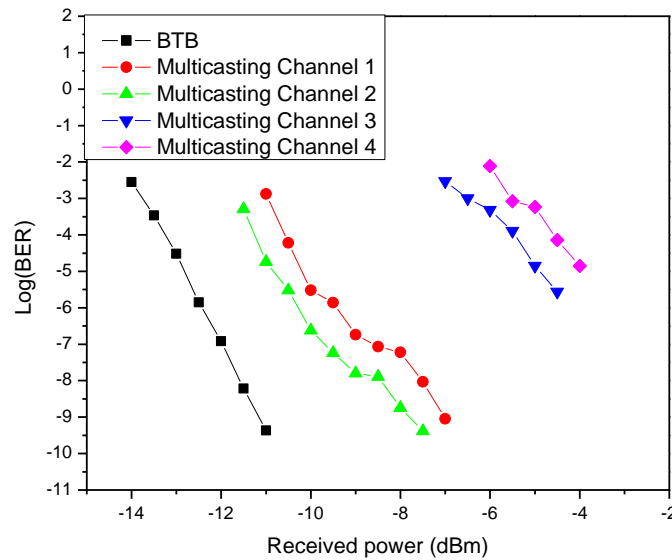


Figure 10: BER versus the received power for 10Gbit/s back-to-back signal and OTDM demultiplexed signal on four wavelength-multicasting channels.

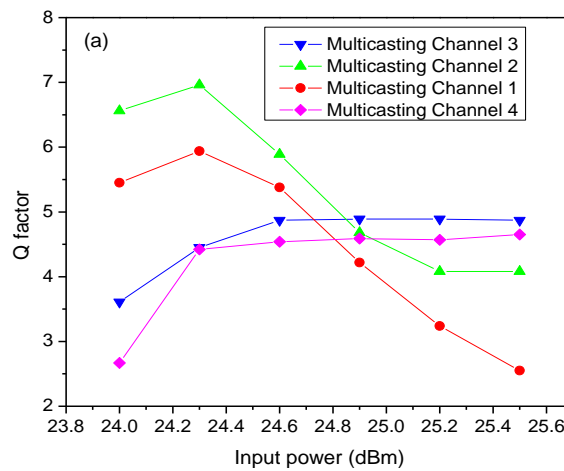


Figure 11: The Q factor of 10Gbit/s wavelength-multicasting signals versus the power of the combined OTDM and control lights input to a 50m DF-HNL-PCF.

A cascaded FWM process requires the sufficiently high powers of lights which are launched into a nonlinear fiber. Due to the limited experimental facilities, we could simply study the operation performance of our designed optical module for OTDM demultiplexing and wavelength multicasting under the conditions of *different optical powers at the input of a 50m DF-HNL-PCF and a fixed spacing (i.e., 6.19 nm) between wavelengths of both OTDM-signal and control-pulse lights*. To achieve this goal, we carry out an experiment in which the power of the combined OTDM and control lights is changed from 24.0 dBm to 25.5 dBm with an increment of 0.3 dB at the DF-HNL-PCF input of our designed module. Then we use a 70GHz electrical sampling oscilloscope cascaded with a 70GHz photodetector to monitor the eye diagram of an OTDM-demultiplexed data signal at 10 Gbit/s on each wavelength multicasting channel. As a result, we can read out the corresponding Q factor of the multicasting signals individually measured by the sampling oscilloscope. Figure 11 shows the variation of the obtained Q factor (from the output of our designed optical module) with the power of the combined OTDM and control lights (input to a DF-HNL-PCF). We can see that the Q factor of all the four multicasting channels is improved as the power of the combined lights is increased from 24.0 dBm to 24.3 dBm. With a further increase of the optical power at the DF-HNL-PCF input, the Q factor of wavelength multicasting channels 1 and 2 is substantially reduced. This is because the multicasting signals at the wavelengths of  $\lambda_{F-1}$  and  $\lambda_{F-2}$  are the first-order FWM components, and they could suffer from a severer crosstalk from the adjacent OTDM and control channels at  $\lambda_s$  and  $\lambda_c$ ,

respectively, if the input optical power of the combined OTDM and control lights at the DF-HNL-PCF exceeds 24.3 dBm to create a stronger FWM effect, as shown in Figure 12. When the input optical power becomes higher than 24.3 dBm, a more significant spectral overlapping between multicasting light 1 (or 2) and OTDM (or control) light is resulted, which effectively degrades the optical signal-to-noise ratio for the multicasting signals at  $\lambda_{F-1}$  and  $\lambda_{F-2}$ . In contrast, the multicasting signals at  $\lambda_{F-3}$  and  $\lambda_{F-4}$  are the second-order FWM products in the cascaded FWM process, and their optical powers can be enhanced with the increase of the power of the combined OTDM and control lights at the DF-HNL-PCF input, while suffering from a severer crosstalk from the adjacent wavelength channels, as shown in Figure 12. Consequently, the Q factor of the multicasting signals at  $\lambda_{F-3}$  and  $\lambda_{F-4}$  is slightly improved, when the input power of the combined OTDM and control lights is increased from 24.3 dBm to 24.6 dBm. However, the corresponding Q factor could be almost unchanged if the optical power of the combined lights is increased from 24.6 dBm to 25.5 dBm at the DF-HNL-PCF input (see Figure 11). It is because a more significant spectral overlapping between multicasting light 3 (or 4) and its adjacent wavelength channel is caused, when the input power of the combined lights becomes higher. In this case, a severer crosstalk is induced on wavelength multicasting channels 3 and 4, while the optical powers of multicasting signals 3 and 4 are also enhanced with the increase of the power of the combined OTDM and control lights at the DF-HNL-PCF input, thus leading to the nearly unchanged Q factor for those two multicasting signals.

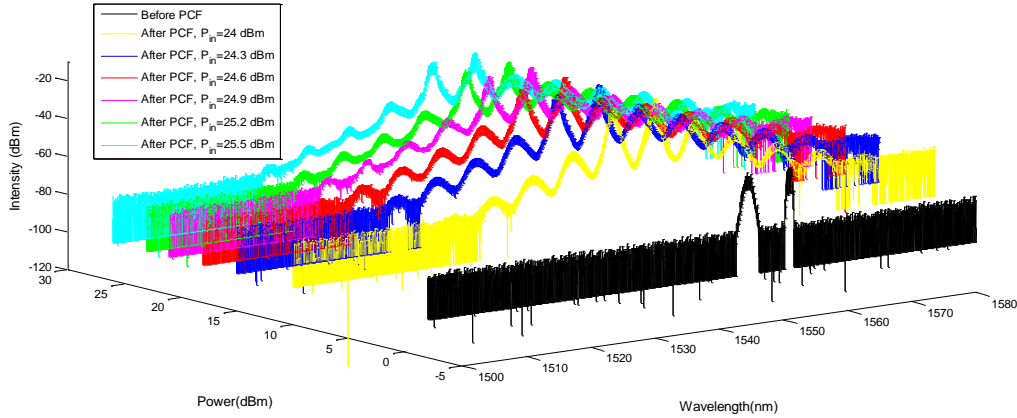


Figure 12: The measured spectra of input and output lights at a 50m DF-HNL-PCF with different input powers of the combined OTDM and control lights.

#### 4. Error-Correcting Code in OTDM System with Simultaneous Time Demultiplexing and Wavelength Multicasting

From the above discussions, one can see that two multicasting signals on wavelength channels 3 and 4 have a high BER at  $10^{-6}$  to  $10^{-5}$ . It is well known that forward-error correction (FEC) is a very powerful technique to combat various noise and interferences in digital communication and computing systems [40]. In [6], Weber *et al* pointed out that the use of a FEC code with 7% overhead was able to efficiently reduce the BERs of all the time-demultiplexed data signals to a level below  $10^{-12}$  in a conventional OTDM transmission system. However, there is no report on the study of using FEC codes to improve the BER performance of OTDM systems with a functionality of simultaneous time demultiplexing and wavelength multicasting. In this section, we propose to employ a FEC code in the newly designed OTDM system to ensure error-free operation on the wavelength-multicasting channels.

Normally, an analytical or simulation approach is often adopted to study the performance improvement of digital optical fiber communication systems with various FEC codes in most of research works, owing to the fact of experimental difficulties associated with testing the full communication performance of a FEC-based digital optical fiber system [41]. Moreover, there is lack of electronic FEC encoder and decoder for use in our experiments. All these make a theoretic study option available only for us to consider. For convenience, we focus our attention on the binary Bose-Chaudhuri-Hocquenghem (BCH) codes in this research work. It is because BCH codes are one of the most important classes of linear block codes for digital communications, and BCH codes also form a large class of powerful cyclic codes with easy implementation based on feedback shift registers and efficient decoding algorithms [40]. Nevertheless, the use of a FEC code leads to increasing the complexity of an OTDM system, since an electronic FEC-code encoder needs to be installed in the front of the electronic data input port of a LiNbO<sub>3</sub> Mach-Zehnder modulator on each OTDM channel and an electronic FEC-code decoder is employed at the output port of an optical receiver on each wavelength-multicasting channel after OTDM demultiplexing. Figure 13 illustrates the schematic diagram of a coded OTDM system with simultaneous time demultiplexing and 1-to- $M$  wavelength multicasting. In effect, both encoder and decoder could operate at a speed being slightly higher than 10 Gbit/s if the original data bit rate is 10 Gbit/s and the binary BCH code with a high code rate is used in such an OTDM system, as will be discussed later. Therefore, those BCH-code encoders and

decoders can be implemented in a cost-effective manner by means of today's mature electronic devices and integrated circuits.

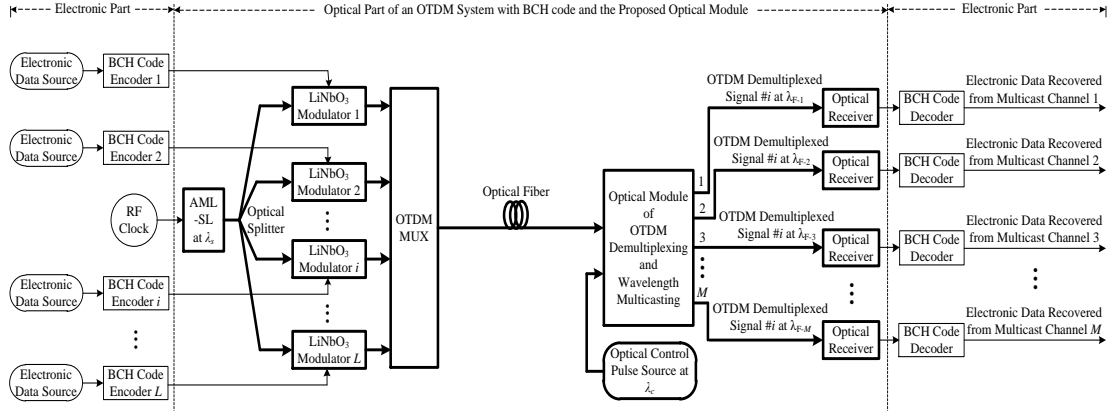


Figure 13: Schematic diagram of an OTDM system with BCH code and functionality of simultaneous time demultiplexing and wavelength multicasting.

At the transmitting end of a coded OTDM system, the  $i$ th electronic BCH-code encoder transforms each input message block of  $k_b$  information bits into a binary codeword of  $n_c$  coded bits (i.e., block length) for  $n_c > k_b$  and  $i = 1, 2, \dots, L$ . The output codewords from this encoder are fed into the  $i$ th LiNbO<sub>3</sub> Mach-Zehnder intensity modulator of the corresponding OTDM channel to produce an optical digital signal based on ultrashort pulses for the subsequent OTDM processing. Then the optical part (indicated in Figure 13) of the coded system is the same as that of an uncoded OTDM system of which the operational principle was already explained in the above sections. At the receiving end of a coded system, the optical data signal on the  $i$ th OTDM channel (for  $i \in [1, L]$ ) is time demultiplexed and is simultaneously multicast over  $M$

wavelength channels which appear individually at  $M$  output ports of an optical module of OTDM demultiplexing and wavelength multicasting (see Figure 13). Then an optical digital receiver is connected with the  $j$ th output port of this optical module to perform the optical-to-electrical conversion and to produce the corresponding electronic data signal, for  $j \in [1, M]$ . At the output of the optical receiver, a BCH-code decoder is employed to decode the received binary codewords in order to recover the electronic data information that was generated by the  $i$ th data source located at the transmitting end. It is known that a  $(n_c, k_b)$  BCH code with the minimum distance  $d_{min}$  can correct  $t$  or fewer errors in any received codeword [40], i.e.

$$t = \left\lfloor \frac{d_{min} - 1}{2} \right\rfloor \quad (2)$$

where the symbol  $\lfloor x \rfloor$  denotes the largest integer less than or equal to  $x$ . Thus, a received codeword could not be decoded correctly if it contains more than  $t$  errors. In other words, the probability of receiving the codeword incorrectly is upper bounded by [40][42]

$$P(E) \leq \sum_{i=t+1}^{n_c} \binom{n_c}{i} p^i (1-p)^{n_c-i} \quad (3)$$

where  $p$  is the transition probability of a binary symmetric channel, i.e.,  $p = p(0|1) = p(1|0)$ . Here  $p(0|1)$  or  $p(1|0)$  is the conditional probability of receiving a bit “0” or “1” when a bit “1” or “0” is transmitted.

Now we can obtain an upper bound on the post-decoding BER of a coded OTDM system by assuming that  $i$  incorrect decoding events produce  $i + t$  post-decoding errors

when  $i > t$ . The post-decoding BER,  $P_{cd}$ , of the coded OTDM system can be thus expressed as [42]

$$P_{cd} \leq \frac{1}{n_c} \sum_{i=t+1}^{n_c} (i+t) \binom{n_c}{i} p^i (1-p)^{n_c-i} \quad (4)$$

Since the code rate  $R$  of a  $(n_c, k_b)$  BCH code is equal to  $k_b/n_c$  for  $k_b < n_c$ , we can appropriately select the parameters  $n_c$  and  $k_b$  to make  $R$  as high as possible, for example,  $R = 0.965$  for a (511, 493) BCH code [40]. If the bit rate of an original electronic data signal is equal to  $B_d$  in an uncoded OTDM system, the BCH-code encoder would produce the coded electronic data signal at a bit rate  $B_{coded} = B_d/R$  ahead of each LiNbO<sub>3</sub> modulator in a coded OTDM system. It is clear that  $B_d$  can be approximate to  $B_{coded}$  when  $R$  is chosen to be close to 1.0, e.g.,  $B_{coded} = 1.04B_d$  for a (511, 493) BCH code. This implies that both coded and uncoded OTDM systems can use the same optical digital receivers of a given bandwidth due to  $B_{coded} \approx B_d$ . In doing so, the BER of each optical digital receiver in an uncoded OTDM system,  $P_{uc}$ , is considered to be equal to that observed at the input of each BCH-code decoder in a coded OTDM system, for a given optical signal power at the input of optical digital receivers. Assume that bits “1” and “0” are equally likely to appear. Then we have  $P_{uc} = 0.5p(0|1) + 0.5p(1|0) = p$ . Substituting it in eq. (4), we can thus establish a relationship between the BERs of both uncoded and coded OTDM systems.

As discussed in the above, we should choose the  $(n_c, k_b)$  binary BCH codes with high  $R$  so as to reasonably compare the BER performance of wavelength-multicasting channels in uncoded and coded OTDM systems. In this case, we consider to use (511, 502) BCH code, (511, 493) BCH code, (511, 484) BCH code, (1023, 1003) BCH code,

(1023, 993) BCH code, and (1023, 983) BCH code [40], as summarized in Table 1 where  $P_{cd}$  is fixed to  $1.0 \times 10^{-9}$  for case I and  $P_{uc}$  is set to  $1.0 \times 10^{-5}$  for case II.

**Table 1:** Use of  $(n_c, k_b)$  Binary BCH Codes to Improve BER Performance of Wavelength-Multicasting Channels in an OTDM System

BCH Code				Uncoded OTDM (Case I)	Coded OTDM (Case I)	Uncoded OTDM (Case II)	Coded OTDM (Case II)
$n_c$	$k_b$	$R$	$t$	$P_{uc}$	$P_{cd}$	$P_{uc}$	$P_{cd}$
511	502	0.982	1	$1.14 \times 10^{-6}$	$1.0 \times 10^{-9}$	$1.0 \times 10^{-5}$	$7.63 \times 10^{-8}$
511	493	0.965	2	$1.67 \times 10^{-5}$	$1.0 \times 10^{-9}$	$1.0 \times 10^{-5}$	$2.16 \times 10^{-10}$
511	484	0.947	3	$7.19 \times 10^{-5}$	$1.0 \times 10^{-9}$	$1.0 \times 10^{-5}$	$3.83 \times 10^{-13}$
1023	1003	0.980	2	$1.05 \times 10^{-5}$	$1.0 \times 10^{-9}$	$1.0 \times 10^{-5}$	$8.63 \times 10^{-10}$
1023	993	0.971	3	$4.27 \times 10^{-5}$	$1.0 \times 10^{-9}$	$1.0 \times 10^{-5}$	$3.08 \times 10^{-12}$
1023	983	0.961	4	$1.06 \times 10^{-4}$	$1.0 \times 10^{-9}$	$1.0 \times 10^{-5}$	$7.88 \times 10^{-15}$

In the case of wavelength multicasting, the BER of a coded OTDM system versus the BER of an uncoded OTDM system is plotted in Figure 14 under the condition of  $B_{coded} \approx B_d$ . We can see that several binary BCH codes of a high code rate can be used in OTDM system with a functionality of simultaneous time demultiplexing and wavelength multicasting to reduce the BERs of the multicasting channels to  $1.0 \times 10^{-9}$ , even though those BCH codes have a relatively small value of  $t$  (i.e.,  $t \leq 3$ ). As discussed in Section 3, an uncoded OTDM system could only achieve the error-free multicasting of the time-demultiplexed signal on the first two wavelength channels at  $\lambda_{F-1}$  and  $\lambda_{F-2}$ ; while the other two multicasting channels at  $\lambda_{F-3}$  and  $\lambda_{F-4}$  suffer from relatively high BERs of  $3.2 \times 10^{-6}$  and  $1.4 \times 10^{-5}$  for the received optical powers of -4.5 dBm and -4

dBm (see Figure 10), respectively. In this case, we can consider to select one of those binary BCH codes with  $t = 2$  or  $3$  from Table 1 and adopt it in such an OTDM system. After post decoding at the receiving end, the BERs of the 3<sup>rd</sup> and the 4<sup>th</sup> wavelength-multicasting channels can be reduced to a level below  $1.0 \times 10^{-9}$ , as shown in Tables 1 and 2. Consequently, the error-free multicasting of an OTDM demultiplexed signal is achieved on all the four wavelength channels. In the real case, once the encoders of a  $(n_c, k_b)$  BCH code are employed at the transmitters of an OTDM system, the coded data signal from the selected OTDM channel is optically time demultiplexed at an optical module of *OTDM demultiplexing & wavelength multicasting* (see Figure 13) and is multicast over all the wavelength channels to reach individual optical receivers. This in turn requires the use of BCH-code decoders at the outputs of all the receivers to recover the data information carried by those multicasting channels, as illustrated in Figure 13. Compared with an uncoded OTDM system achieving the error-free multicasting on wavelength channels 1 and 2, the input powers of the multicast optical data signals can be substantially lowered down at two receivers on wavelength channels 1 and 2 of the coded OTDM system while still maintaining the  $\text{BER} \leq 1.0 \times 10^{-9}$ . In doing so, this can also improve the power budget for the corresponding wavelength channels. For example, we can use the (1023, 1003) BCH code in an OTDM system to increase the power budgets by more than 3 dB on wavelength channels 1 and 2, respectively, as shown in Table 2.

**Table 2:** Use of Binary BCH Codes with  $t = 2$  or 3 for Error-Free Multicasting of OTDM-demultiplexed Signal on Four Wavelength Channels

	Wavelength-Multicasting Channels					
	# 1	# 2	# 3	# 4	# 1	# 2
Received Power	-7Bm	-7.5dBm	-4.5dBm	-4dBm	-10dBm	-10.5dBm
Measured $P_{uc}$	$1.0 \times 10^{-9}$	$4.2 \times 10^{-10}$	$3.2 \times 10^{-6}$	$1.4 \times 10^{-5}$	$3.1 \times 10^{-6}$	$3.2 \times 10^{-6}$
Theoretical $P_{cd}$ for BCH (511, 493)	n/a	n/a	$7.08 \times 10^{-12}$	$5.91 \times 10^{-10}$	$6.44 \times 10^{-12}$	$7.08 \times 10^{-12}$
Theoretical $P_{cd}$ for BCH (511, 484)	n/a	n/a	$3.97 \times 10^{-15}$	$1.47 \times 10^{-12}$	$3.65 \times 10^{-15}$	$3.97 \times 10^{-15}$
Theoretical $P_{cd}$ for BCH (1023, 1003)	n/a	n/a	$2.84 \times 10^{-11}$	$2.36 \times 10^{-9}$	$2.58 \times 10^{-11}$	$2.84 \times 10^{-11}$
Theoretical $P_{cd}$ for BCH (1023, 993)	n/a	n/a	$3.24 \times 10^{-14}$	$1.18 \times 10^{-11}$	$2.87 \times 10^{-14}$	$3.24 \times 10^{-14}$

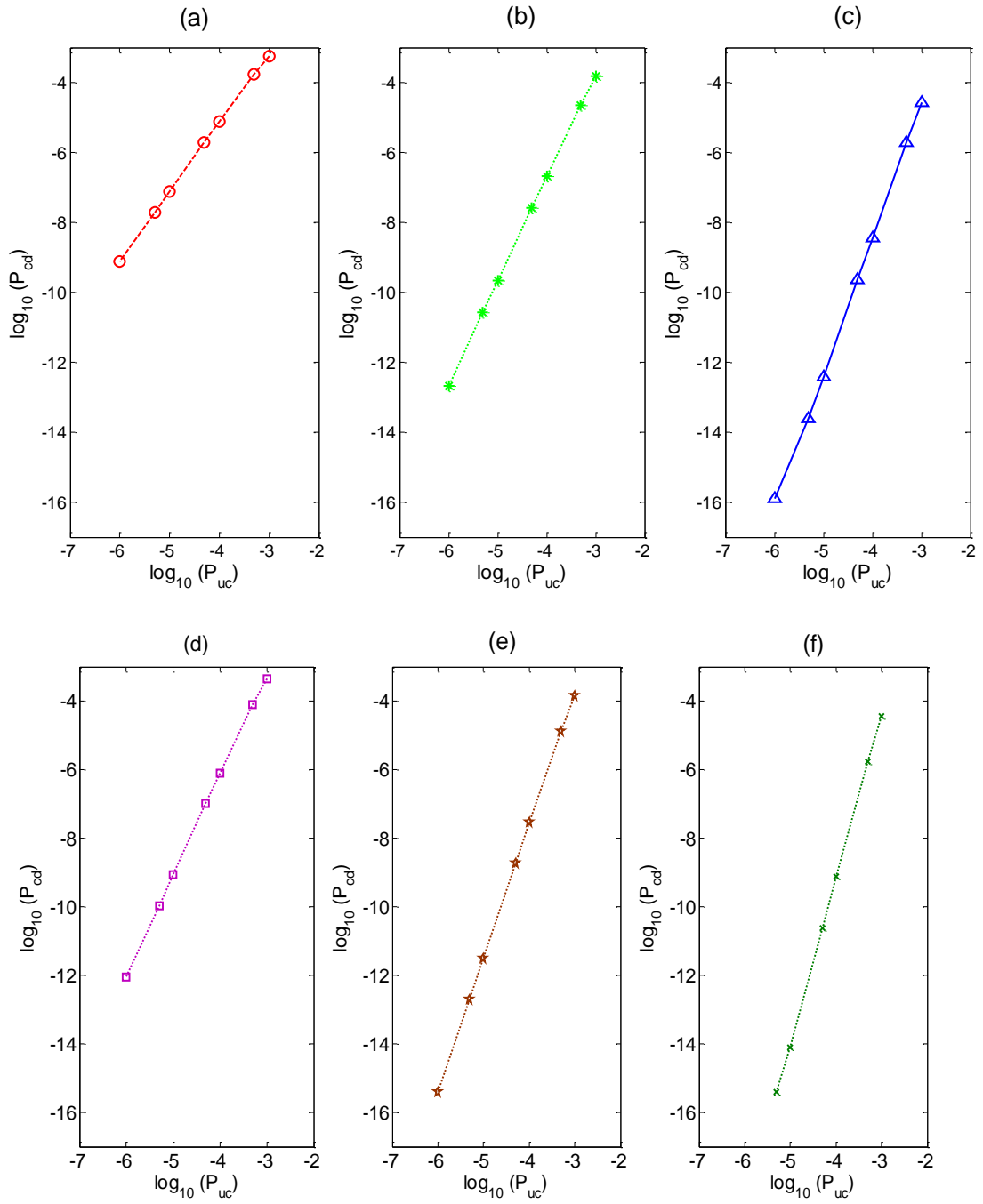


Figure 14: BER of a coded OTDM system versus BER of an uncoded OTDM system under the condition of  $B_{coded} \approx B_d$ . (a) (511, 502) BCH code, (b) (511, 493) BCH code, (c) (511, 484) BCH code, (d) (1023, 1003) BCH code, (e) (1023, 993) BCH code, and (f) (1023, 983) BCH code, respectively.

## 5. Conclusions

We have reported a new design of OTDM systems in this paper. A functionality of simultaneous time demultiplexing and wavelength multicasting is achieved by employing the cascaded FWM in a DF-HNL-PCF, while the multicasting performance of such an OTDM system is improved by using the scheme of forward-error correction. The proposed system has a simple configuration and requires only a single control-pulse light source for simultaneous OTDM demultiplexing and wavelength multicasting. A key component to realize our designed OTDM system is called the module of *OTDM demultiplexing and wavelength multicasting*. Moreover, we have experimentally demonstrated the 100Gbit/s-to-10Gbit/s OTDM demultiplexing together with 1-to-4 wavelength multicasting. In the experiment, we used a 3dB optical coupler, a high-power EDFA, a 50m DF-HNL-PCF, a 1×4 optical splitter, and 4 OBPFs to implement a module of *OTDM demultiplexing and wavelength multicasting*, but this module would be simplified if a 1×4 optical splitter and 4 OBPFs are replaced by a suitable wavelength demultiplexer. The control-pulse light was generated in our experiment by the wavelength conversion of a 10GHz optical clock pulse train through supercontinuum generation in a dispersion-shifted HNLF. Our experimental results have shown that error-free wavelength multicasting is achieved on two wavelength channels with the minimum power penalty of 3.2 dB relative to the 10Gbit/s back-to-back measurement, whereas the BERs of other two multicasting channels are measured to be at the level of  $10^{-6}$  to  $10^{-5}$ . In this case, we have proposed the use of  $(n_c, k_b)$  binary BCH codes of high code rate to improve the multicasting performance of the designed OTDM system. Our work has revealed that the resulting system can theoretically support error-free multicasting of the OTDM-demultiplexed signal on four wavelength channels by employing those BCH codes with  $t = 2$  or 3.

## Acknowledgement

This work is supported by the Chinese Academy of Sciences (CAS)/SAFEA International Partnership Program for Creative Research Teams, the National Nature Science Fund of China (Number: 61201193), and the Shaanxi Province Science and Technology Research and Development Program (Number: 2014k05-40). The authors wish to thank the State Key Laboratory of Transient Optics and Photonics at the Xi'an Institute of Optics and Precision Mechanics of CAS for supporting the experimental research work.

## References

1. G. Wellbrock and T.J. Xia, "2010 The road to 100G deployment," *IEEE Communications Magazine*, vol. 48, no. 3, pp. s14-18, Mar. 2010.
2. A.E. Willner, S. Khaleghi, M.R. Chitgarha, and O.F. Yilmaz, "All-optical signal processing," *J. Lightwave Technol.*, vol. 32, no. 4, pp. 660-680, Feb. 2014.
3. H. Hu, P. Munster, E. Palushani, M. Galili, H.C.H. Mulvad, P. Jeppesen, and L.K. Oxenlowe, "640 GBd phase-correlated OTDM NRZ-OOK generation and field trial transmission", *J. Lightwave Technol.*, vol. 31, no. 4, pp. 696-701, Feb. 2013.
4. L.K. Oxenlowe, M. Galili, H.C. Hansen Mulvad, H. Hu, J.I. Areal, E. Palushani, H. Ji, A.T. Clausen, and P. Jeppesen, "Nonlinear optical signal processing for Tbit/s Ethernet applications," *International Journal of Optics*, vol.2012, pp.573843-56, 2012.
5. H.C. Hansen Mulvad, M. Galili, L.K. Oxenlowe, H. Hu, A.T. Clausen, J.B. Jensen, C. Peucheret, and P. Jeppesen, "Demonstration of 5.1 Tbit/s data capacity on a single-wavelength channel," *Optics Express*, vol. 18, no. 2, pp. 1438-1443, Feb. 2010.
6. H.G. Weber, S. Ferber, M. Kroh, C. Schmidt-Langhorst, R. Ludwig, V. Marembert, C. Boerner, F. Futami, S. Watanabe, and C. Schubert, "Single channel

- 1.28 Tbit/s and 2.56 Tbit/s DQPSK transmission,” *Electronics Letters*, vol. 42, no. 3, pp. 178-179, Feb. 2006.
7. M. Nakazawa, T. Yamamoto, and K.R. Tamura, “1.28Tbit/s-70km OTDM transmission using third- and fourth-order simultaneous dispersion compensation with a phase modulator,” *Electronics Letters*, vol. 36, no. 24, pp. 2027-2029, Nov. 2000.
  8. E. Tangdiongga, Y. Liu, H. de Waardt, G.D. Khoe, and H.J.S. Dorren, “2006 320-to-40-Gb/s demultiplexing using a single SOA assisted by an optical filter,” *IEEE Photon. Technol. Lett.*, vol. 18, no. 8, pp. 908-910, Apr. 2006.
  9. S. Diez, R. Ludwig, and H.G. Weber, “All-optical switch for TDM and WDM/TDM systems demonstrated in a 640Gbit/s demultiplexing experiment,” *Electronics Letters*, vol. 34, no. 8, pp.803-805, Apr.1998.
  10. J. Li, B.-E. Olsson, M. Karlsson, and P.A. Andrekson, “OTDM demultiplexer based on XPM-induced wavelength shifting in highly nonlinear fiber,” *IEEE Photon. Technol. Lett.*, vol. 15, no. 8, pp.1770-1772, Dec. 2003.
  11. E.J.M. Verdurmen, Y. Zhao, E. Tangdiongga, J.P. Turkiewicz, G.D. Khoe, and H. de Waardt, “Error-free all-optical add-drop multiplexing using HNLF in a NOLM at 160 Gbit/s,” *Electronics Letters*, vol.41, no.6, pp. 349-350, Mar. 2005.
  12. W. Wang, L. Rau, H.N.Poulsen, and D.J.Blumenthal, “Raman gain enhanced FWM 160Gb/s OTDM demultiplexer withhighly-nonlinear-fiber,” in *Proc. 2004 Optical Fiber Communication Conference (OFC2004)*, Paper ThN3, 2004.
  13. A.I. Siahlo, L.K. Oxenlowe, K.S. Berg, A.T. Clausen, P.A. Andersen, C. Peucheret, A. Tersigni, P. Jeppesen, K.P. Hansen, and J.R. Folkenberg, “A high-speed demultiplexer based on a nonlinear optical loop mirror with a photonic crystal fiber,” *IEEE Photon. Technol. Lett.*, vol.15, no.8, pp.1147-49, Aug. 2003.
  14. A.S. Lenihan, R. Salem, T.E. Murphy, and G.M. Carter, “All-optical 80-Gb/s time-division demultiplexing using polarization-insensitive cross-phase modulation in photonic crystal fiber,” *IEEE Photon. Technol. Lett.*, vol.18, no.12, pp.1329-1331, Jun. 2006.
  15. K. Igarashi, K. Katoh, K. Kikuchi, T. Nagashima, T. Hasegawa, S. Ohara, and N. Sugimoto, “160-Gbit/s optical time-division demultiplexing based on cross-phase modulation in a 2-m-long dispersion-shifted Bi<sub>2</sub>O<sub>3</sub> photonic crystal fiber,” in *Proc. QELS'07, (Paper JTuC3, 2007) 2007*

16. C.-S. Bres, A.O.J. Wiberg, B.P.-P. Kuo, J.M. Chavez-Boggio, C.F. Marki, N. Alic, and S. Radic, "Optical demultiplexing of 320 Gb/s to 8×40 Gb/s in single parametric gate," *J. Lightwave Technol.*, vol.28, no.4, pp.434-442, Feb. 2010.
17. Z.-Q. Hui and J.-G. Zhang, "Wavelength conversion, time demultiplexing and multicasting based on cross-phase modulation and four-wave mixing in dispersion-flattened highly nonlinear photonic crystal fiber," *J. Opt.*, vol.14 ,no.5, pp.055402, May. 2012.
18. L.K. Oxenløwe, H. Ji, M. Galili, M. Pu. H. Hu, H.C.H. Mulvad, K. Yvind, J.M. Hvam, A.T. Clausen, and P. Jeppesen, "Silicon photonics for signal processing of Tbit/s serial data signals," *IEEE Journal of Selected Topics in Quantum Electronics*, vol.18, no.2, pp. 996-1005, Mar./Apr. 2012
19. M. Galili, J. Xu, H.C.H. Mulvad, L.K. Oxenlowe, A.T. Clausen, P. Jeppesen, B. Luther-Davies, S. Madden, A. Rode, D.-Y. Choi, M. Pelusi, F. Luan, and B.J. Eggleton, "Breakthrough switching speed with an all-optical chalcogenide glass chip: 640 Gbit/s demultiplexing," *Opt. Express*, vol.17, no.4, pp.2182-2187, Feb. 2009.
20. W.H. Reeves, J.C. Knight, P.St.J. Russell, and P.J. Roberts, "Demonstration of ultra-flattened dispersion in photonic crystal fibers," *Opt. Express*, vol.10, no.14, pp. 609-613, Jun. 2002.
21. K.P. Hansen, "Dispersion flattened hybrid-core nonlinear photonic crystal fiber," *Opt. Express*, vol.11, no.13, pp.1503-1509, Jun. 2003.
22. P.A. Andersen, T. Tokle, Y. Geng, C. Peucheret, and P. Jeppesen, "Wavelength conversion of a 40-Gb/s RZ-DPSK signal using four-wave mixing in a dispersion-flattened highly nonlinear photonic crystal fiber," *IEEE Photon. Technol. Lett.*, vol.17, no.9, pp. 1908-1910, Sep. 2005.
23. K.K. Chow, C. Shu, C. Lin, and A. Bjarklev, "All-optical wavelength multicasting with extinction ratio enhancement using pump-modulated four-wave mixing in a dispersion-flattened nonlinear photonic crystal fiber," *IEEE Journal of Selected Topics in Quantum Electronics*, vol.12, no.4, pp.838-842, Jul/Aug. 2006.
24. A.G. Coelho, Jr., M.B.C. Costa, A.C. Ferreira, M.G. da Silva, M.L. Lyra, and A.S.B. Sombra, "Realization of all-optical logic gates in a triangular triple-core

- photonic crystal fiber”, *J. Lightwave Technol.*, vol. 31, no. 5, pp. 731-739, March 2013.
25. M.P. Fok and C. Shu, “Multipump four-wave mixing in a photonic crystal fiber for  $6 \times 10$  Gb/s wavelength multicasting of DPSK signals,” *IEEE Photon. Technol. Lett.*, vol.19, no.15, pp.1166-1168, Aug. 2007.
  26. R.T. Murray, E.J.R. Kelleher, S.V. Popov, A. Mussot, A. Kudlinski, and J.R. Taylor, “Widely tunable polarization maintaining photonic crystal fiber based parametric wavelength conversion”, *Optics Express*, vol. 21, no. 13, pp. 15826-15833, July 2013.
  27. J.P. Mack, T.U. Horton, W. Astar, K.J. Ritter, and G.M. Carter, “Polarization insensitive wavelength conversion by FWM of multiformat DWDM signals using birefringent PCF”, *IEEE Journal of Selected Topics in Quantum Electronics*, vol. 18, no. 2, pp. 909-915, March/April 2012.
  28. Y. Wang, C. Yu, T. Luo, L. Yan, Z. Pan, and A.E. Willner, “Tunable all-optical wavelength conversion and wavelength multicasting using orthogonally polarized fiber FWM,” *J. Lightwave Technol.*, vol.23, no.10, pp.3331-3338, Oct. 2005.
  29. H.-F. Ting, K.-Y. Wang, J.R. Stroud, A.C. Foster, and M.A. Foster, “Efficient wavelength multicasting through four-wave mixing with a comb source”, in *Technical Digest of 2014 CLEO*, paper STu2I.5, San Jose, California, USA, 8-13 June 2014.
  30. T. Kurosu, K. Solis-Trapala, and S. Namiki, “Phase-regenerative multicasting of BPSK signals by hybrid optical phase squeezer”, in *Proc. OECC/ACOFT 2014*, pp. 996-998, Melbourne, Australia, 6-10 July 2014.
  31. Z.-Q. Hui, J.-G. Zhang, “Demonstration of 100Gbit/s optical time-division demultiplexing with 1-to-4 wavelength multicasting by using the cascaded FWM in photonic crystal fiber with a single control light source,” *Microwave and Optical Technology Letters*, vol.56, no.10, pp.2330-2335, Oct. 2014.
  32. G.P. Agrawal, *Fiber-Optic Communication Systems*, 3<sup>rd</sup> ed. John Wiley & Sons, New York, 2002.

33. T.T Ng, J.L. Blows, J.T. Mok, R.W. McKerracher, and B.J. Eggleton, "Cascaded four-wave mixing in fiber optical parametric amplifiers: Application to residual dispersion monitoring," *J. Lightwave Technol.*, vol.23, no.2, pp.818-826, Feb. 2005.
34. A. Cerqueira S. Jr, J.M. Chavez Boggio, A.A. Rieznik, H.E. Hernandez-Figueroa, H.L. Fragnito, and J.C. Knight, "Highly efficient generation of broadband cascaded four-wave mixing products," *Optics Express*, vol.16, no.4, pp.2816-28, Jan. 2008.
35. A. Cerqueira S. Jr, J.M. Chavez Boggio, A.A. Rieznik, H.E. Hernandez-Figueroa, and H.L. Fragnito, "Broadband generation of cascaded four-wave mixing products," in *Proc. 2007 SBMO/IEEE MTT-S International Microwave and Optoelectronics Conference (IMOC 2007)* 550-553, 2007.
36. C.J. McKinstrie, M.G. Raymer, "Four-wave-mixing cascades near the zero-dispersion frequency," *Optics Express*, vol.14, no.21, pp.9600-9610, Oct. 2006.
37. X. Liu, R.M. Osgood Jr, Y.A. Vlasov, and W.M.J. Green, "Mid-infrared optical parametric amplifier using silicon nanophotonic waveguides," *Nature Photonics*, vol.4, no.8, pp.557-560, Aug. 2010.
38. H.C. Hansen Mulvad, E. Tangdiongga, H. de Waardt, and H.J.S. Dorren, "40 GHz clock recovery from 640 Gbit/s OTDM signal using SOA-based phase comparator," *Electronics Letters*, vol. 44, no. 2, pp. 146-147, Jan. 2008.
39. F. Gomez-Agis, L.K. Oxenlowe, S. Kurimura, C. Ware, H.C. Hansen Mulvad, M. Galili, and D. Erasme, "Ultrafast phase comparator for phase-locked loop-based optoelectronic clock recovery systems," *J. Lightwave Technol.*, vol. 27, no. 13, pp. 2439-2448, July 2009.
40. S. Lin and D.J. Costello, Jr., *Error Control Coding*, 2<sup>nd</sup> ed. Pearson Prentice Hall, Upper Saddle River, New Jersey, USA, 2004.
41. R.-J. Essiambre, G. Kramer, P.J. Winzer, G.J. Foschini, B. Goebel, "Capacity limits of optical fiber networks," *J. Lightwave Technol.*, vol.28, no.4, pp.662-701, Feb. 2010.
42. J.-G. Zhang, "Performance improvement of fibre-optic code-division multiple-access systems by using error-correction codes," *IEE Proc.-Commun.* vol.144, no.5, pp.316-321, Oct. 1997.